Biophysical Journal, Volume 98

Supporting Material

Understanding the Concentration Dependence of Viral Capsid Assembly Kinetics - the Origin of the Lag Time and Identifying the Critical Nucleus Size

Michael F. Hagan and Oren M. Elrad

Supporting Information for: Understanding the Concentration Dependence of Viral Capsid Assembly Kinetics - the Origin of the Lag Time and Identifying the Critical Nucleus Size

Michael F. Hagan and Oren M. Elrad

I. BROWNIAN DYNAMICS SIMULATIONS DETAILS

Lag times were measured following the procedure described in Fig. 3, with completion fractions as a function of time averaged over up to 600 independent simulations at each subunit volume fraction. For simulations with volume fractions $v_0 \leq 0.006$, obtaining a statistically relevant measurement of the lag time according to the procedure described in Fig. 3 becomes computationally challenging, due to the low nucleation rate. Specifically, it is difficult to estimate the location and value of the maximal assembly rate due to noise. This limitation was overcome by fitting a pre-assumed form for the completion fraction (the CNT model) to the simulation measurements. As our intention was to obtain as accurate an estimate of the lag times possible, rather than to determine whether or not the CNT model is consistent with the simulation results, we used f_0 and c_0 as fitting parameters independently for each subunit concentration. While it is beyond the scope of the present work, a global fit of the CNT model to the simulation data would enable a useful test of some model assumptions.

The crossover point c_c shown in Fig. 1b was calculated according to Eq. 5, with the initial nucleation rate $\tau_{\rm nuc}^{\rm min}$ estimated by measuring the nucleation rate as a function of the free subunit concentration in the steady-state ensemble simulations.

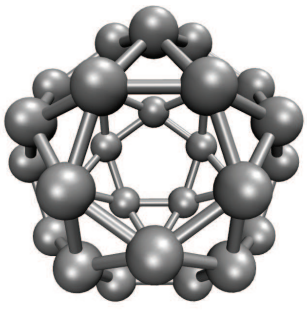

FIG. 6: The capsid geometry in the Brownian dynamics simulation model is comprised of 30 subunits (each of which represents a protein dimer) in an icosahedral shell. The center of each subunit roughly corresponds to a 2-fold axis of symmetry (at dimer interfaces) in a T=1 capsid (e.g. see Ref. [1] and the VIPER database [2]). Subunit sizes are reduced to aid visibility.

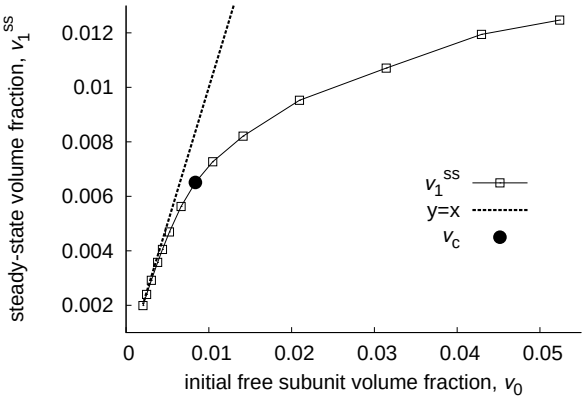

FIG. 7: The steady-state volume fraction calculated from the steady-state ensemble simulations is shown as a function of the total subunit volume fraction v_0.

II. CALCULATING ELONGATION RATES WITH INTERMEDIATE-DEPENDENT FORWARD RATE CONSTANTS

For the CNT model and the extended NG model considered next, the forward rate constants are proportional to the perimeter of the partial capsid intermediate, $f_n = f_0 l_n$, with the perimeter $l_n = 2[\pi n(N-n)/N]^{1/2}$. In the limit $fc_1 \gg b_{\rm elong}$ we can calculate the average capsid size $n(t)$ as a function of time

$$\frac{dn(t)}{dt} = f[n(t)] - b[n(t)] \approx f_0 \frac{4\pi R}{N} \left[N(n(t)-N)\right]^{1/2} \tag{10}$$

where f_n is written as $f[n(t)]$ to emphasize that we have temporarily taken the continuum limit. We have neglected $b[n(t)]$ in the approximate equality on the right and assumed $N \gg n_{\rm nuc}$. This expression can be integrated to give $n(t) = N\sin^2(f_0 t/2R)$, which can be inverted to yield the average elongation time

$$\tau_{\rm elong} = 0.5(\pi N)^{1/2}/(f_0 c_1) \tag{11}$$

In Fig. 5 and Fig. 8, we see that elongation times for the CNT model and the extended NG model can be approximated with Eq. 2 by setting $f = 2f_0(N/\pi)^{1/2}$.

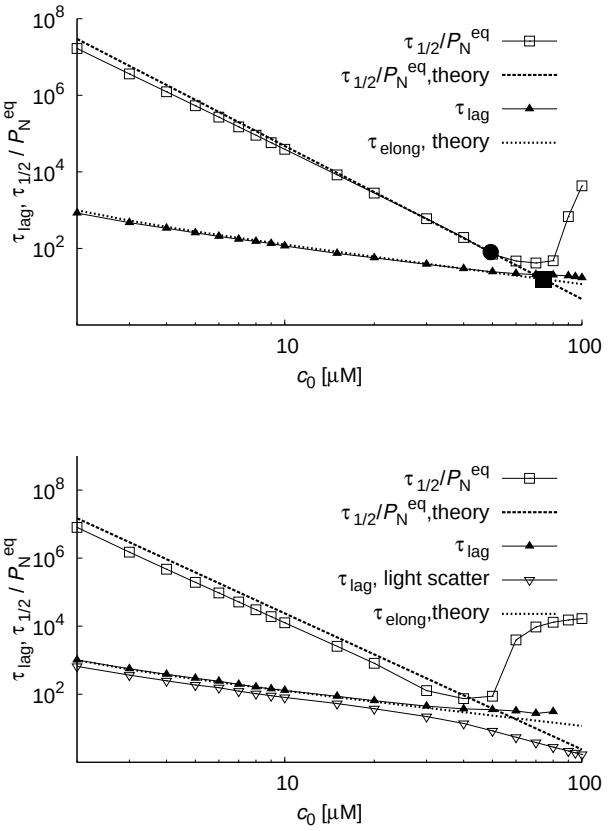

FIG. 8: **(a)** Numerical results for the NG model with intermediate-dependent association rate constants. The median assembly times $\tau_{1/2}$ and the lag times $\tau_{\rm lag}$ calculated from the completion fraction ($P_{\rm N}$) and calculated light scatter ($I_{\rm LS}$) are shown as functions of initial subunit concentration c_0 (the light scatter results closely track the completion fraction as in Fig. 4). The estimates for the median assembly time (Eq. 4 with $n_{\rm nuc} = 5$) and lag time (Eqs. 2 and 11) are shown as dashed lines, and the estimates for the crossover concentration $c_{\rm c}$ and kinetic trap concentration $c_{\rm kt}$ (Eq. 5) are shown as symbols (defined as in Fig. 4). **(b)** Numerical and theoretical estimates are shown for median assembly times, and lag times are compared to the theoretical estimate of the elongation time, for the NG model extended to enable association of dimers with partial-capsid intermediates.

III. EXTENDING THE NG MODEL TO ACCOUNT FOR INTERMEDIATE-DEPENDENT RATE CONSTANTS AND BINDING OF OLIGOMERS

In this section we consider two alterations to the NG model to further evaluate if our conclusions are model dependent. **Intermediate-dependent association rate constants.** First, we relax the assumption that the association rate constant is independent of intermediate size by setting the forward rate constant as in the CNT model, $f_n = f_0 l_n$, with $f_0 = 10^5/[2(N/\pi)^{1/2}]$. As for the CNT model, the numerically calculated lag times for this model agree quite well with the theoretical estimate of Eq. 2 (Fig. 8a). The estimated median assembly time $\tau_{1/2}$ calculated with Eq. 4 using $f = f_0 l_4$ shows reasonable agreement with the numerical results, but over a smaller range of concentrations than for the original NG model. The discrepancy at low concentrations may occur because the effective nucleation rate slowly varies with concentration, or may be due to error in the numerical integration at large times. We note that the scaling predicted by Eq. 4 holds over the range of subunit concentrations that can be studied experimentally. This observation shows that a slight generalization of the NG model to include two association rate constants can be made equivalent to this model. Because the average elongation rate constant is faster than the nucleation rate constant in this model, the crossover point $c_{\rm c}$ moves to a slightly higher concentration than for the NG model, but still occurs roughly at the concentration for which $\tau_{\rm elong} = \tau_{\rm nuc}^{\rm min}$ (Eq. 5).

Association of oligomers. We also consider a version of the NG model in which dimers associate(dissociate) to(from) intermediates with the same rate constant as monomers. As shown in Fig. 8b, the quantitative values for lag times and median assembly times change under this condition, but the scaling for both observables is unchanged. Although we did not explicitly calculate $c_{\rm c}$ or $c_{\rm kt}$ for this model, we note that the crossover behavior still begins at the concentration for which initial nucleation rates are equal to the elongation time.

IV. THE SLOW APPROACH TO EQUILIBRIUM

The fraction of subunits in capsids $P_{\rm N}(t)$ is shown as a function of initial subunit concentration c_0 at various times in Fig. 9.

V. ESTIMATING THE MEDIAN ASSEMBLY TIME

In this section we derive an approximate expression for the median assembly time $\tau_{1/2}$, or the time at which the reaction is 50% complete: $P_{\rm N}(\tau_{1/2}) = 0.5 P_{\rm N}^{\rm eq}$. We begin by considering an irreversible reaction that proceeds according to n$^{\rm th}$ order nucleation kinetics

$$\frac{dc}{dt} = -N k_{\rm nuc} c^n \tag{12}$$

with c the time-dependent concentration of free subunits and $k_{\rm nuc}$ the nucleation rate constant. The factor N accounts for the fact that N subunits are depleted for each capsid that forms. Integrating Eq. 12 yields

$$\frac{c(t)}{c_0} = \left[(n-1) N k_{\rm nuc} c_0^{n-1} t + 1\right]^{\frac{-1}{n-1}} \tag{13}$$

with $c_0 = c(0)$. The median assembly time for this irreversible reaction corresponds to $c(\tau_{\rm irrev}) = 0.5 c_0$ which gives

$$\tau_{\rm irrev} = \frac{2^{n-1} - 1}{(n-1) N k_{\rm nuc}} c_0^{-(n-1)}. \tag{14}$$

To approximately account for the effect of back reactions on the assembly time scale, we apply the standard formula for

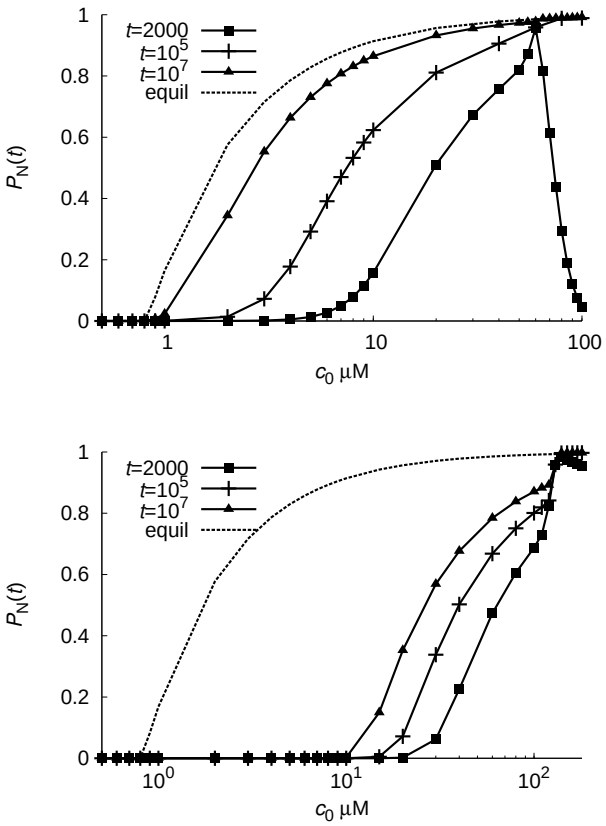

FIG. 9: Completion fractions at indicated times are shown as functions of initial subunit concentration c_0 for **(a)** the nucleation and growth model and **(b)** the classical nucleation model. In **(a)** and **(b)**, the kinetic trap points $c_{\rm kt}$ corresponds to the maximum in $P_{\rm N}$ with respect to c_0 at $t = 2000$.

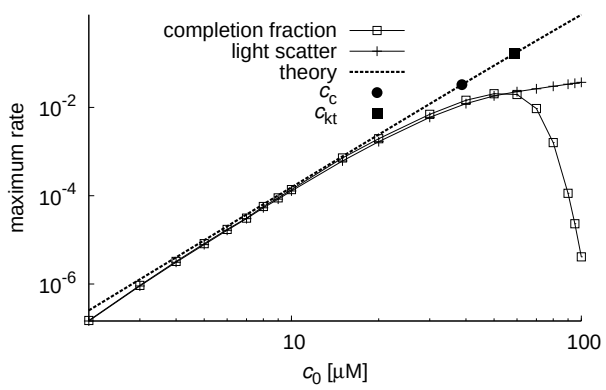

FIG. 10: The maximum assembly rates calculated from the completion fraction ($P_{\rm N}$) and calculated light scatter ($I_{\rm LS}$) are shown as functions of initial subunit concentration c_0. The theoretical estimate for the maximum nucleation rate ($1/\tau_{\rm nuc}^{\rm min}$ calculated from Eq. 3 with $n_{\rm nuc} = 5$) is shown as a dashed line.

two-state kinetics, which relates the overall reaction timescale τ to the forward reaction rate k according to $\tau = P^{\rm eq}/k$, with $P^{\rm eq}$ the fraction reacted at equilibrium. To arrive at Eq. 4 we substitute $P_{\rm N}^{\rm eq} = P^{\rm eq}$ and $1/k = \tau_{\rm irrev}$.

VI. MAXIMUM ASSEMBLY RATES

The maximum assembly rates are shown as a function of the initial subunit concentration in Fig. 10.

[1] R. W. Lucas, S. B. Larson, and A. McPherson, J. Mol. Biol. **317**, 95 (2002).

[2] P. Natarajan, G. C. Lander, C. M. Shepherd, V. S. Reddy, C. L. Brooks, and J. E. Johnson, Nat. Rev. Microbiol. **3**, 809 (2005).